A potential deduced from low energy $^{16}O(\alpha,\alpha)$ elastic scattering

F. Michel*
Faculté des Sciences, Université de Mons-Hainaut, B-7000 Mons, Belgium

G. Reidemeister
Physique Nucléaire Théorique et Physique Mathématique, Université Libre de Bruxelles, CP229, B-1050 Bruxelles, Belgium

Y. Kondō
Department of Natural Sciences, Kyoto Women's University, Kyoto 605, Japan
(Received 2 February 1995)

The properties of the $\alpha+^{16}O$ interaction in the vicinity of the Coulomb barrier are investigated by constructing (real, energy-independent) potentials which reproduce — when resonant nonpotential contributions are added to the potential background — all available $^{16}O(\alpha,\alpha)$ elastic scattering angular distributions and excitation functions between 3.5 and 9 MeV incident energies. These low energy potentials, which are constructed for angular momenta ranging from 0 to 5, are in line with the global potential extracted from the analysis of the higher energy data ($20 \leq E_\alpha \leq 150$ MeV), but a slight angular momentum dependence, and an increase of the barrier height of about 1 MeV, are found necessary to reproduce the low energy data; this effect is qualitatively similar to that predicted by calculations taking into account antisymmetrization or dispersion relation effects. These potentials reproduce the properties of the first three members of the ^{20}Ne $K^\pi = 0_4^+$ "higher nodal" rotational band, which dominate the scattering in the investigated energy range, and of the $J^\pi = 5^-$ member of the $K^\pi = 0^-$ "inversion doublet" band. By taking into account the energy dependence of the interaction at lower energy, these potentials also give a nice account of the properties of the $J^\pi = 1^-$ and 3^- members of the same band, and are found to be compatible with the properties of the first three members of the ^{20}Ne ground state band.

PACS number(s): 21.60.Gx, 24.10.Ht, 25.55.Ci, 27.30.+t

I. INTRODUCTION

The investigation of the properties of the nucleus-nucleus interaction in the vicinity of the Coulomb barrier has focused considerable interest in the recent years [1–4], in connection with the so-called "threshold anomaly" seen in elastic scattering, and with the enhancement of the fusion cross sections observed at low energies (see Ref. [1], and references therein). Most of these studies concentrate on heavy-ion systems where transfer reactions and the excitation of collective modes are thought to be instrumental in enhancing fusion at energies near or below the top of the barrier. The threshold anomaly, which manifests itself by a rapid increase of the strength of the real part of the optical potential when energy decreases, could be linked to the fusion enhancement since it results in a decrease of the potential barrier height, which in turn could reflect dynamical polarization effects induced in the one-channel optical potential by, e.g., transfer reactions. This conjecture is partly supported by explicit coupled-channel calculations. Another, more global, line of attack is provided by the so-called dispersion relation approach [5–7], where the effect of the opening of all nonelastic channels above the threshold on the real part of the optical model potential is treated by taking into account the energy behavior of the empirical imaginary potential. It is not yet completely clear if this contribution is attractive or repulsive in the barrier region relative to potentials at energies above the barrier since its detailed radial behavior depends on the parametrization of the energy behavior of the imaginary potential [7]. On the other hand, microscopic calculations of the resonating group method (RGM) [8–10] or fishbone model [11, 12] types — mainly carried out for the $\alpha+^{16}O$ system — indicate that antisymmetrization effects are also likely to induce rapid changes in the potential strength in the barrier region as the incident energy decreases.

The observation of threshold effects is generally difficult in the case of heavy-ion scattering since the interaction is dominated at low energy by Coulomb excitation, and thus by a very long-range polarization potential [13], which tends to mask the specific nuclear effects. Also potentials extracted from the analysis of heavy-ion elastic scattering data are generally poorly determined, since the latter essentially fixes the potential strength around the so-called strong absorption radius, making a detailed extraction of energy dependencies of the potential rather problematic. A rather indirect evidence is provided by the fact that the renormalization constant used in simple models like the folding model frequently varies rapidly

*Electronic address: sniche@vm1.umh.ac.be

with the incident energy around the Coulomb barrier [14]. The clearest evidence for a threshold effect is displayed by the behavior of integrated quantities like volume integrals or other moments of the potential [7], which tend to be determined with better accuracy than the individual potential parameters, and which are known with reasonable accuracy for lighter, more transparent systems like $^{12}C + ^{12}C$ [1]. Even in these cases the low-energy data are plagued with the discrete ambiguity phenomenon, and one must invoke continuity arguments to follow the potential from the high energies down to the Coulomb barrier region [15]. Whatever the accuracy attained, changes in the potential shape seem to remain out of reach of these empirical studies. Other indirect, and also more model-dependent, indications for threshold anomalies in the potential rely on the analysis of inelastic or transfer reactions or of anomalous fusion.

In view of the importance of a clear understanding of the dynamics of the nucleus-nucleus interaction, and of its implications for a correct description of inelastic, transfer, and fusion processes, it is worth striving to extract the most precise possible information [16] on the (presumably few) systems where strong absorption does not hamper a quantitative determination of the potential. Clearly heavy-ion systems are ruled out from this respect, and even light-ion scattering like α-particle scattering is rarely adequate since even in this case the optical potential is generally not known on sufficiently broad radial and energy ranges. Of course, conclusions drawn from such light-ion systems should not be extended without caution to more massive ones; for example dispersion relation effects, whose importance grows when the opening of nonelastic channels becomes more rapid [1], are likely to be larger for heavy-ion systems where many such channels are available when the incident energy reaches the top of the Coulomb barrier. At the same time, nonlocality effects should lose their importance since their range is expected to become small as compared to the radius of the interaction potentials [17]. However a clear evidence for an energy dependence of the potential shape in light-ion scattering could be a very useful test for the various models available [16].

One of the most interesting systems for exploring the low-energy behavior of the nucleus-nucleus interaction is the $\alpha + ^{16}O$ system, which was studied some time ago by the present authors from this point of view [18]. One of its decisive advantages lies in the fact that because of the doubly-closed shell nature of the partners, the first inelastic thresholds are substantially higher than the top of the Coulomb barrier ($V_B \simeq 4$ MeV). Therefore when the incident energy reaches the top of the barrier, the scattering remains purely elastic, and even after crossing the first inelastic threshold (which occurs at $E_\alpha \simeq 7.5$ MeV), absorption effects remain negligible up to about 10 MeV incident energy since a phase shift analysis using purely real phase shifts proved to be feasible up to that energy [19].

Furthermore, the absorption remains comparatively low even at higher energies, causing the well-known anomalous large angle scattering (ALAS) phenomenon, and making possible a precise determination of a unique global optical potential from about 20 to 146 MeV incident energy [20]. This potential, which is weakly energy-dependent, was substantiated quantitatively by microscopic RGM-WKB calculations [21, 22]. Its low-energy properties are similar to those of the folding potential built by Buck *et al.* [23] to describe the properties of the bound and quasibound cluster states of ^{20}Ne. Its real part binds a number of unphysical states with a principal quantum number $N = 2n + \ell < 8$ [20], which in an orthogonality condition model (OCM)-type interpretation correspond to the so-called forbidden states of the RGM for that system and are therefore to be discarded, and physical states which group into rotational bands characterized by principal quantum numbers $N = 8$, 9, and 10, which correspond to the well-known $K^\pi = 0_1^+, 0^-$, and 0_4^+ α-cluster bands in ^{20}Ne [23, 24]. A recent reanalysis of Abele and Staudt [25] including new measurements essentially confirmed the results of the global analysis of Ref. [20].

In Ref. [18], the low energy properties of the $\alpha + ^{16}O$ potential were extracted by analyzing the high precision data of Buser [26], extending on the whole angular range between $E_\alpha = 3.5$ and 4.9 MeV. It was shown in that study that a quantitative description of these data could only be reached provided (i) the interaction potential is made slightly angular-momentum dependent; indeed angular-momentum independent potentials cannot reproduce the near-degeneracy of the two broad $J^\pi = 0^+$ and 2^+ resonances ($\Gamma \simeq 1$ MeV) (which correspond to the first two members of the 0_4^+ band) found by McDermott *et al.* [27] around 4.9 and 5.1 MeV incident energy, respectively, and whose low-energy tails dominate the scattering data of Buser; (ii) the nuclear interaction is made less attractive in the surface region with respect to that needed at higher energy, making the barrier significantly higher at these low energies.

Another more recent study [25], carried out within the folding model approach, essentially confirmed the first result of [18], but a renormalization of the barrier height was not found necessary in describing the low-energy data. This (apparent) discrepancy prompted us to resume our original analysis, extending it on the broadest energy range possible, and trying to estimate its possible model dependencies. We found that a consistent analysis of the available elastic scattering data from 3.5 to 9 MeV laboratory energy makes possible a rather unambiguous determination of an $\alpha+^{16}O$ interaction potential for angular momenta ℓ ranging from 0 to 5. This potential displays a significant enhancement of the barrier height, which tends to decrease with increasing ℓ. In addition it gives a nice account of the ^{20}Ne rotational bands which have the $\alpha+^{16}O$ (g.s.) cluster structure.

The results of our new analysis are presented in Sec. II. A brief summary and our conclusions appear in Sec. III.

II. POTENTIAL ANALYSIS OF THE DATA UP TO 9 MeV INCIDENT ENERGY

A. Phase shifts

As stressed in the Introduction, $\alpha + ^{16}O$ scattering remains essentially elastic up to about 10 MeV incident

energy. Indeed the first inelastic threshold, which corresponds to the excitation of the $J^\pi = 0^+$, $E_x = 6.05$ MeV state in ^{16}O, is only reached at $E_\alpha \simeq 7.5$ MeV, and even above that energy it proves possible to reproduce the existing angular distributions and excitation functions in a phase shift analysis using purely real phase shifts up to about 10 MeV incident energy [19]. This phase shift analysis aimed at extracting the parameters (energies, widths) of the numerous resonances observed in the studied energy range, and it complements an earlier analysis of McDermott *et al.* [27] between 3.7 and 6.5 MeV. Above 10 MeV the fits of John *et al.* [19] deteriorate rapidly, pointing to the need of using complex phase shifts, which was not attempted in that paper in view of the ambiguities which affect this type of multiparameter analyses. Below 10 MeV a parametrization with phase shifts up to $\ell = 6$ was found to be sufficient to fit the data.

The more recent measurements of Buser [26] between 3.5 and 4.9 MeV made possible the extraction of the $\ell = 0$ to $\ell = 3$ phase shifts, which connect smoothly to those of John *et al.* [19] at 5 MeV and agree reasonably well with the solution of McDermott *et al.* [27] (note that in the latter work the quantities displayed include a hard sphere contribution, which must be subtracted before being compared with Buser's phase shifts). The angular distributions of Buser are dominated by the low-energy tail of two very broad resonances with $\ell = 0$ and $\ell = 2$, which were also observed by McDermott *et al.* [27] and are now interpreted [24] as corresponding to the first two members, with $J^\pi = 0^+$ and 2^+, of the $K^\pi = 0_4^+$ higher nodal band in ^{20}Ne. The broad $\ell = 4$ resonance observed at $E_\alpha \simeq 7.6$ MeV [19] is thought to be the third member of the same band. The $\ell = 1$ and $\ell = 3$ phase shifts, except for a few isolated resonances, are essentially smooth and close to 180° at low energy, and they decrease slowly with the incident energy. This can be interpreted as an "echo" behavior of these phase shifts, which display sharp resonances at energies slightly below the lower energy end of Buser's data, that is at $E_\alpha = 1.3174$ and 3.0382 MeV, respectively [28]. These two resonances, with c.m. widths of 28 eV and 8.1 keV, respectively, are associated with the first two $J^\pi = 1^-$ and 3^- members of the $K^\pi = 0^-$ "inversion doublet" band in ^{20}Ne [29,24]. The $J^\pi = 5^-$ member of this band manifests itself as an isolated resonance in the $\ell = 5$ phase shift [19] at $E_\alpha = 6.912$ MeV ($\Gamma_{\text{c.m.}} = 141$ keV).

As all the states mentioned above are thought to have the $\alpha + {}^{16}$O (g.s.) cluster structure (the excitation of the members of the $K^\pi = 0_4^+$ band with respect to those of the ^{20}Ne g.s. band is a radial excitation), they should be describable — as well as the part of the scattering which is not contaminated by "outside" resonances with different underlying structure — in terms of a purely real potential since only the radial degree of freedom of the relative motion is active. The real part of the unique global optical potential of Ref. [20], which reproduces the higher-energy ^{16}O(α,α) elastic scattering data between 32.2 and 146.0 MeV incident energy and which will be denoted hereafter as the A_0 potential, was indeed found, after a slight renormalization of its depth, to be able to reproduce the energy location as well as the essential properties (widths, electromagnetic transition probabilities) of these cluster states with good accuracy [30]. It also gives a qualitative reproduction of the data of Buser; the energies of the latter are far from any of the sharp resonances found at lower [31] and higher [27] energy, which thus have negligible influence on the scattering. However, it was shown in Ref. [18] that a quantitative reproduction of these data required, as recalled in the Introduction, the inclusion of a slight angular momentum dependence and of a substantial modification of the surface behavior of the A_0 potential.

To gain a more quantitative impression of the phase shifts the purely potential approach should reproduce, it proves very useful to subtract from the total experimental phase shifts the "nonpotential" resonance contributions. This was made by subtracting from these phase shifts simple Breit-Wigner contributions:

$$\delta_\ell = \arctan \frac{\Gamma}{2(E_R - E)}, \tag{1}$$

with parameters E_R and Γ taken directly from the literature [27,19]. Of course the resonances corresponding to the $\alpha + {}^{16}$O (g.s.) cluster states mentioned above should not be included in this subtraction procedure. We note that the effects linked to the interference of nearby resonances with the same spin are ignored, as they were also in the above-mentioned studies for extracting the resonance level parameters. The result of this subtraction is presented in Fig. 1 (dots). The original phase shifts [19] were actually carefully extracted from the original figures by a scanning and digitizing procedure. It should be noted that the fluctuations seen in some subtracted phase shifts do not prevent the extraction of a meaningful average behavior. These fluctuations have essentially two origins; indeed for very sharp resonances, small errors in the scanning/digitizing treatment can have dramatic effects, as can have slight deviations of the resonance parameters of the literature with respect to optimal values. The only example where we compensated for this last effect by a fine tuning of the experimental resonance energy is that of the $J^\pi = 4^+$, $E_R = 6.569$ MeV resonance [19], where changing the resonance energy to 6.600 MeV significantly reduced the excursions of the subtracted $\ell = 4$ phase shift with respect to a smooth average behavior. It is also worth emphasizing that the broad $J^\pi = 0^+$, $E_R = 7.8$ MeV resonance of John *et al.* [19], with its c.m. width of 576 keV, gives a non-negligible contribution of several degrees to the $\ell = 0$ phase shift down to energies as low as 4 MeV, which is difficult to accept from a physical point of view. Therefore, this contribution was subtracted only from the experimental phase shifts of Ref. [19]; at the energies of Buser [26], which are far from any other significant resonance contribution, the phase shifts which appear in Fig. 1 are thus the original phase shifts of Ref. [26].

B. The global A_0 potential

The A_0 potential can in fact be extrapolated to lower energies, and it was shown [20] to be able to reproduce

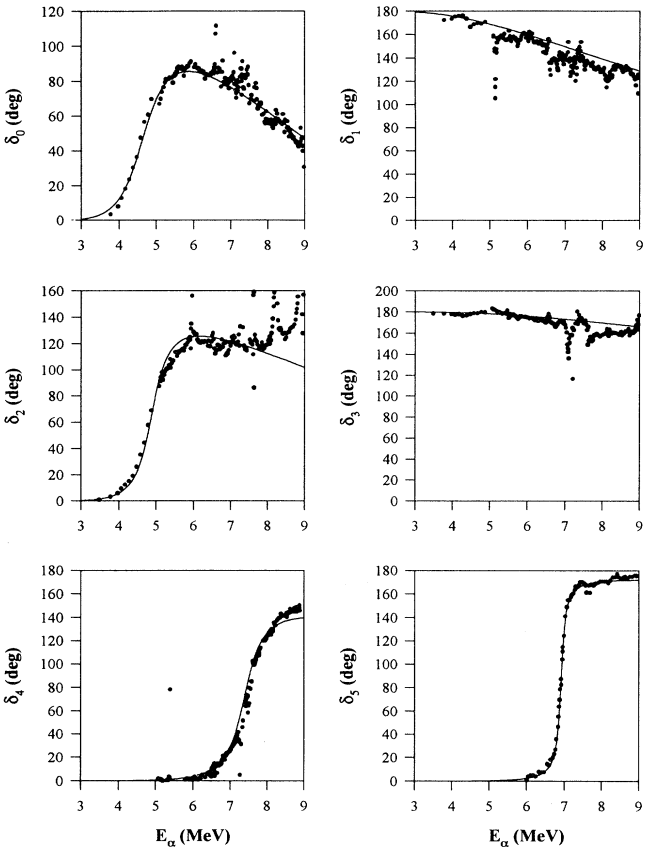

FIG. 1. Experimental $^{16}O(\alpha,\alpha)$ subtracted phase shifts [19, 26] (dots, see text) and potential model predictions obtained with the parameters of Table II (solid lines).

the average behavior of the fluctuating excitation functions of Refs. [32, 33] between 15 and 30 MeV with reasonable accuracy. It reads

$$V(r) = V_C(r) - U(r) - iW(r)$$
$$= V_C(r) - \frac{U_0\left\{1+\alpha\exp\left[-(r/\rho)^2\right]\right\}}{\left\{1+\exp\left[(r-R_R)/2a_R\right]\right\}^2}$$
$$-i\frac{W_0}{\left\{1+\exp\left[(r-R_I)/2a_I\right]\right\}^2}. \quad (2)$$

Despite its somewhat complicated appearance, all its parameters are fixed, except α and R_I which vary smoothly and control its energy behavior on the whole 20–146 MeV energy range. In Eq. (2), V_C denotes the Coulomb potential due to a uniformly charged sphere of radius $R_C = 1.3\ A^{1/3}$ fm = 3.276 fm, and the fixed parameters assume the values $U_0 = 38$ MeV, $R_R = 4.3$ fm, $a_R = 0.6$ fm, $\rho = 4.5$ fm, $W_0 = 25$ MeV, and $a_I = 0.65$ fm. This remarkable global potential is thus able [20] to reproduce the transition between low-energy scattering, where intermediate structure effects are still apparent, to energies where this structure disappears and where the scattering is dominated by a vigorous ALAS behavior (typically between about 30 and 50 MeV), and finally to the energies where ALAS fades out and disappears to leave a pure rainbow scattering regime [34]. It was shown [20] that this global potential is characterized by a particularly low absorption, which makes possible a precise determination of its real part down to unusually small distances; indeed for most α + nucleus systems, absorption is significantly stronger than in the case of nucleon scattering, and the potential is essentially determined only in the surface region around the so-called strong absorption radius. This particularly low absorption is undoubtedly due to the doubly closed-shell nature of both the projectile and target; α particles accessing the nuclear interior thus have a non-negligible chance to escape back into the entrance channel, and thus they carry information on this part of the potential, the more so as the contribution corresponding to a reflection at the barrier and that due to the wave entering the nuclear interior [35] display strong interference effects in the angular region where they are of similar magnitude [20]. Another system which strikingly displays ALAS and the same type of internal-barrier wave interference around 30 MeV incident energy is the α + ^{40}Ca system, which was the first case where an optical model interpretation of ALAS was shown to be viable [36], and where the crucial importance of the internal wave contribution to this effect — and thus the nuclear interior transparency — was demonstrated [37]. The properties of the global potential of Ref. [20] have been amply confirmed by the recent reanalysis of the $^{16}O(\alpha,\alpha)$ angular distributions between 32 and 146 MeV, including several new measurements, within the frame of the folding model approach [25]. In particular, the volume integrals per nucleon pair

$$j_U = 4\pi\int_0^\infty r^2U(r)dr/4A \quad (3)$$

of the real part of the folding potentials, which are adjusted at each energy through a normalization parameter λ, do not differ by more than a few percent from those of Ref. [20], and the quality of the fits obtained is quite similar.

The reason why, even after tuning the parameter α which controls the real well depth of the A_0 potential, and even after making it angular momentum dependent, the quality achieved by the fits to Buser's data is still unsatisfactory [18] can be understood by inspecting the energy behavior of the phase shifts generated by the A_0 potential for various values of α, and comparing them with the subtracted phase shifts of Fig. 1; this is made in Fig. 2(a) for the case of the $\ell = 0$ phase shift, which resonates around $E_\alpha = 4.5$ MeV with a width $\Gamma \simeq 1$ MeV. It can be seen that using the value of α assumed by the A_0 potential at $E_\alpha = 32.2$ MeV, that is $\alpha = 3.407$, leads to a width which is close to the experimental value, since the maximum slopes of the experimental and calculated phase shifts are similar; however, the calculated $\ell = 0$ resonance is seen to fall about 1 MeV too low. On the other hand, although reducing the potential depth by decreasing the value of α brings the resonance energy in better agreement with experiment, the calculated width is now much larger than that of its experimental counterpart [see Fig. 2(a)]. Of course the energy behavior of the

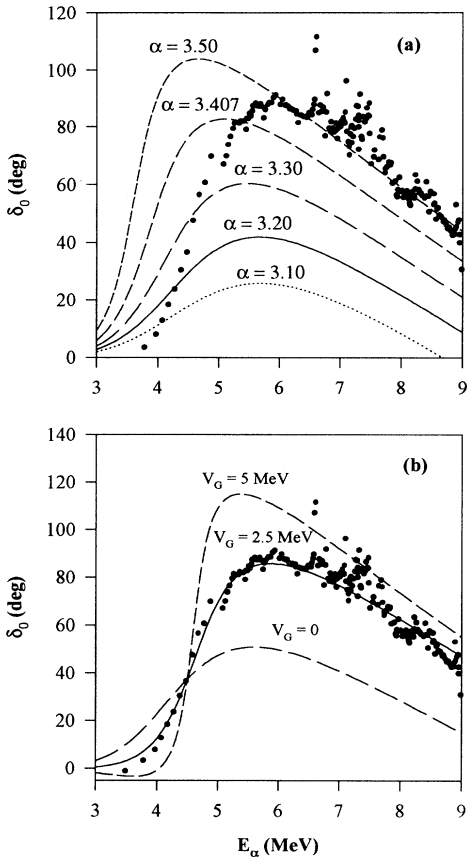

FIG. 2. (a) $\ell = 0$ experimental subtracted phase shift (dots) and the predictions of the A_0 potential for various values of the strength parameter α. (b) Same as (a), but the A_0 potential is now supplemented with a surface repulsive Gaussian term of strength V_G located at $R_G = 5.5$ fm.

experimental phase shift can be reproduced artificially by making the depth of the potential (and thus the parameter α) strongly energy dependent; indeed inspection of Fig. 2(a) shows that making α jump from about 3.10 to 3.50 when E_α rises from 4 to 6 MeV would make possible a nice reproduction of the experimental phase shift. However such a drastic energy dependence is difficult to accept from a physical point of view, since it corresponds to an excursion of some 25 MeV fm^3 of the volume integral per nucleon pair of the potential on the small 2 MeV range considered here, a value much higher than the predictions of current models based on dispersion relation [7] or on nonlocality effects [9, 2] (typical changes of the volume integrals per nucleon pair expected from these effects do not exceed about 2 to 3 MeV fm^3 per MeV). This remark helps to understand the apparent discrepancy between the studies of Refs. [18] and [25], where the increase of the barrier height found in the former was not found necessary in the latter. Examination of the energy behavior of the normalization parameter λ used in the folding model analysis of Ref. [25] indeed shows that this parameter is systematically and rapidly increasing between 3.5 and 5.0 MeV, especially for $\ell = 0$ where the volume integral of the real potential rises by more than 30 MeV fm^3. As the form factor of the folding model potential is by itself nearly energy independent on this energy scale (the only source of energy dependence originates from the one-nucleon exchange contribution contained in the N-N interactions used, which all derive from the M3Y effective interaction), it is difficult to accept that the folding model "explains" the low-energy data without having to introduce some extra mechanism like, e.g., an additional potential barrier.

C. Increase of the barrier height

The effect of introducing such a barrier is clearly illustrated in Fig. 2(b). Instead of modifying the geometry of the original A_0 potential by changing the value of its diffuseness parameter a_R to enhance the barrier, as was done in Ref. [18], which has the unwanted side effect of modifying not only the surface but also the internal behavior of the potential at the same time, we chose to add explicitly a repulsive Gaussian term:

$$\Delta V(r) = V_G \exp\left\{-\left[(r - R_G)/a_G\right]^2\right\} \tag{4}$$

located in the surface region of the potential; the internal part of the potential can be adjusted independently by tuning the parameter α. To avoid the use of an excessive number of parameters, the centroid R_G and width a_G of this Gaussian repulsion were fixed at the values 5.5 and 1.5 fm, respectively (these values lead to a potential modification similar to that used in Ref. [18]), the only variable parameter being the strength V_G. Figure 2(b) shows the effect on the $\ell = 0$ phase shift of adding to the bare potential ($V_G = 0$, $\alpha = 3.25$) Gaussians of strength $V_G = 2.5$ and 5 MeV (with values of α leading to equal values of δ_0 at the energy of the resonance, $E_\alpha \simeq 4.5$ MeV); it is seen that a repulsive term of about 2.5 MeV brings the calculation in nearly perfect agreement with the "experimental" subtracted phase shift. The effect of such a modification on the effective (nuclear + Coulomb) $\ell = 0$ potential is presented in Fig. 3; the potential barrier top, which had a height (calculated with the $E_\alpha = 32$ MeV A_0 potential, thick solid line) of some 3 MeV, is now seen to have risen by about 1 MeV (thin solid line).

One may of course wonder to what extent this result is "model independent," that is, how it depends on the parametrization assumed for the additional repulsive potential. This point was investigated by refitting the theoretical $\ell = 0$ phase shift generated by the modified potential used in Fig. 2(b) (with $V_G = 2.5$ MeV) between 3.5 and 9 MeV, using Gaussian repulsive potentials with different values of R_G; the parameters V_G, a_G, and α were readjusted independently for each value of R_G. An excellent reproduction of this phase shift, and thus of the experimental subtracted phase shift, were obtained for values of R_G ranging from 4 to 6 fm in steps of 0.5 fm; beyond 6 fm the quality of the fits deteriorates rapidly. The values of the parameters obtained, together with the volume integrals of the corresponding potentials, are listed in Table I, and the corresponding $\ell = 0$ effective po-

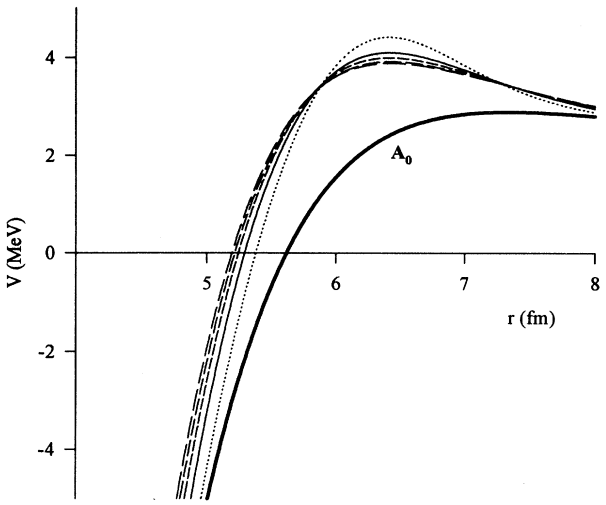

FIG. 3. Comparison of the $\ell = 0$ effective potential barrier generated by the $E_\alpha = 32.2$ MeV A_0 potential (thick solid line) and by modified potentials with Gaussian repulsive barriers located at values of R_G ranging from 4 (long dashed line) to 6 fm (dotted line) in 0.5 fm steps (see text).

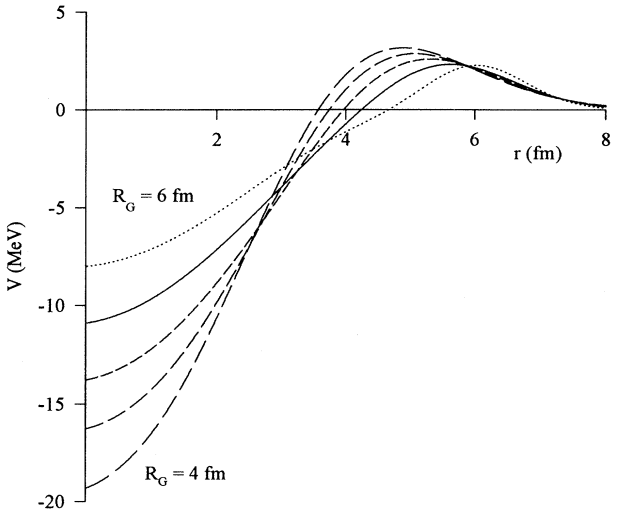

FIG. 4. Difference between the potentials, with different values of R_G, fitting the subtracted $\ell = 0$ phase shift, and the $E_\alpha = 32.2$ MeV A_0 potential (same conventions as in Fig. 3).

tential barriers appear in Fig. 3. The latter show very little scatter, and examination of Table I shows that the parameters of the Gaussian repulsive potentials readjust themselves when R_G is varied so as to preserve the height and location of the top of the effective potential barrier at the values $V_B \simeq 4$ MeV, $R_B \simeq 6.4$ fm, which therefore appear to be determined rather model independently by the data. At the same time it is seen that the volume integrals of the potentials obtained do not vary strongly when the location of the repulsive term is varied.

It is also interesting to have a look at the total modification of the potential implied by these modifications. This is displayed in Fig. 4, which shows that the difference between the potentials obtained and the original $E_\alpha = 32$ MeV A_0 potential is essentially repulsive beyond about 4 fm and attractive in the internal region. Whereas the location and height of the top of the barrier are determined with good accuracy by the data (the curves of Fig. 4 are very similar beyond 5.5 fm, in the vicinity of R_B), it appears that there exists some compensation between the internal ($r < 3$ fm) and intermediate ($3 < r < 5$ fm) parts of the potential, which are therefore determined with lower accuracy.

TABLE I. Parameters of the Gaussian modification reproducing the $\ell = 0$ phase shift for different locations R_G; j_U is the volume integral per nucleon pair of the total potential.

R_G (fm)	V_G (MeV)	a_G (fm)	α	j_U (MeV fm^3)
4.0	4.77	2.27	3.95	369.8
4.5	3.73	2.05	3.86	373.5
5.0	3.02	1.80	3.79	377.4
5.5	2.50	1.50	3.71	380.8
6.0	2.34	1.09	3.63	383.2

The stability of the results obtained prompted us to pursue our analysis within the same frame, that is by adding a repulsive Gaussian term for each ℓ value to the $E_\alpha = 32$ MeV A_0 potential, keeping R_G and a_G fixed at the values 5.5 and 1.5 fm, respectively, and adjusting V_G and α in order to get the best possible agreement with each of the subtracted phase shifts active in the studied energy range ($E_\alpha = 3.5 - 9$ MeV), that is for $\ell \leq 5$. Some energy dependence of the potential should in principle be introduced on this extended energy range, but part of this effect is probably taken into account by the explicit ℓ dependence of the potential. Indeed the energy range where each phase shift varies rapidly is, even for broad resonances, substantially less than the 6 MeV range investigated here, and adjusting the energy location and width of each of these resonances by tuning the potential parameters turns out to be more than adequate for describing the empirical phase shifts. In addition letting the potential depend on both the energy and angular momentum would unavoidably lead to ambiguous parameters. The results of our adjustment appear in Fig. 1 as solid lines, while the corresponding parameters, together with the associated volume integrals, are summarized in Table II.

TABLE II. Parameters and volume integrals per nucleon pair of the potentials reproducing the "experimental" subtracted $\ell = 0$ to $\ell = 5$ phase shifts (see text).

ℓ	α	V_G (MeV)	j_U (MeV fm^3)
0	3.71	2.5	380.8
1	3.50	1.0	389.6
2	3.81	2.0	396.5
3	3.50	1.0	389.6
4	3.87	2.0	401.0
5	3.238	0.5	378.1

Examination of Table II reveals two striking features. The first one is the progressive decrease of the strength of the repulsion V_G needed to reproduce the subtracted phase shifts as a function of ℓ. This was in a sense expected, since the energy where a particular phase shift is active tends to increase with ℓ, and the potential should converge towards the A_0 potential around 20 MeV incident energy. More unexpected is the fact that this strength is manifestly parity dependent, V_G being smaller for the odd-parity waves than for the even-parity ones. It must be noted that in our previous study [18], which extended on the much smaller $E_\alpha = 3.5$ to 4.9 MeV range, these effects could not be seen since a common surface radial behavior was assumed for all ℓ values, the diffuseness parameter a_R taking the ℓ-independent value 0.372 fm. This did not provide an optimal reproduction of the $\ell = 0$ phase shift, but in view of the small energy range covered, and of the negligible influence of the $\ell = 4$ and of the odd partial waves on this range (see Fig. 1), use of this common geometry was found sufficient to obtain a nice reproduction of Buser's data [26]. The most important ingredients in this success turn out to be the introduction of a slight ℓ dependence of the internal part of the potential (essentially to reproduce the near-degeneracy of the $\ell = 0$ and $\ell = 2$ phase shifts mentioned above) and an (ℓ-independent) increase of the barrier height. The first of these effects has recently been confirmed by the folding model analysis of Ref. [25]. As for the volume integrals, they are seen to depend rather weakly on ℓ, the most notable exception being that of the $\ell = 0$ potential which assumes a rather small value in order to reproduce the experimental near degeneracy of the $\ell = 0$ and $\ell = 2$ phase shifts. The volume integrals we obtain are in fact in nearly complete agreement with those obtained by Abele and Staudt [25] in the middle of the range of Buser's data; at $E_\alpha = 4.477$ MeV for example, they obtain $j_U = 380.6$, 386.3, 396.5, and 386.3 MeV fm^3 for $\ell = 0$ to 3, respectively, to be compared with our corresponding values 380.8, 389.6, 396.5, and 389.6 MeV fm^3.

D. Elastic scattering data and $K^\pi = 0^-$ and 0_4^+ cluster bands

Since the parametrization obtained reproduces well the subtracted "experimental" phase shifts between 3.5 and 9 MeV incident energies, and thus, after adding the nonpotential resonance contributions of Eq. (1), also reproduces the full experimental phase shifts, it should give a good account of the experimental elastic angular distributions and excitation functions available in this energy range. Figure 5 shows, for example, how the excitation functions of McDermott *et al.* [27] are reproduced by the present approach (solid lines). In Fig. 5, the dashed lines represent the potential contribution to the full cross section. It is seen that below $E_\alpha \simeq 5$ MeV, the nonpotential resonances play a negligible role in the scattering, and indeed the angular distributions of Buser between 3.5 and 4.9 MeV could be well reproduced in a purely potential

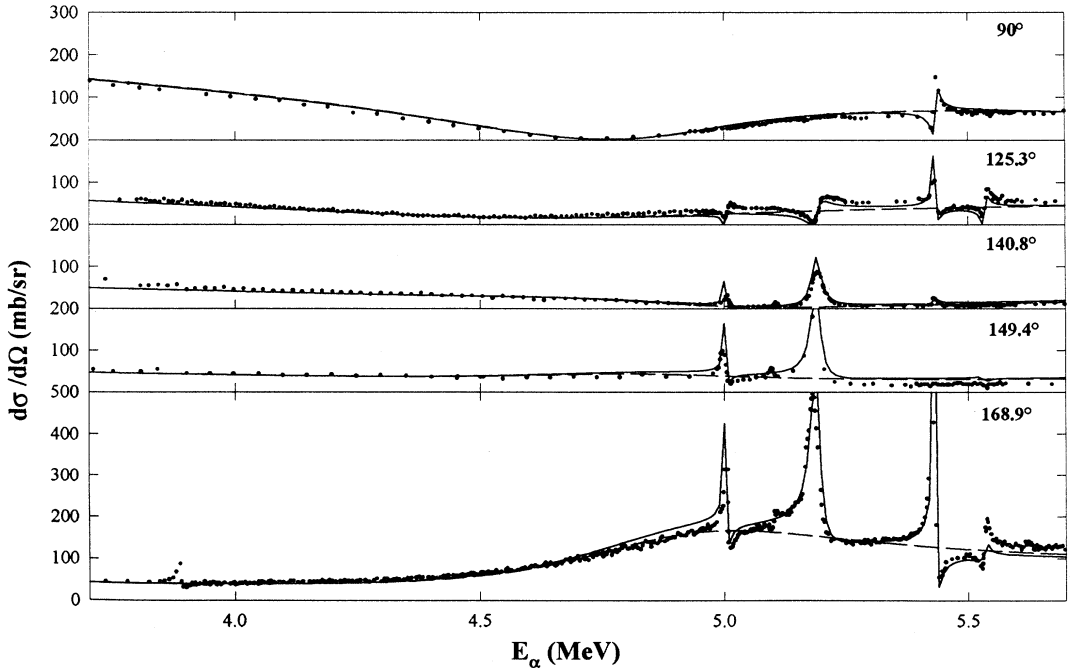

FIG. 5. Comparison of the predictions of the potential model + nonpotential resonances (solid lines) with the elastic scattering excitation functions of McDermott *et al.* [27] at $\theta_{\text{c.m.}} = 90$, 125.3, 140.8, 149.4, and 168.9° (dots); the dashed lines present the pure potential contribution.

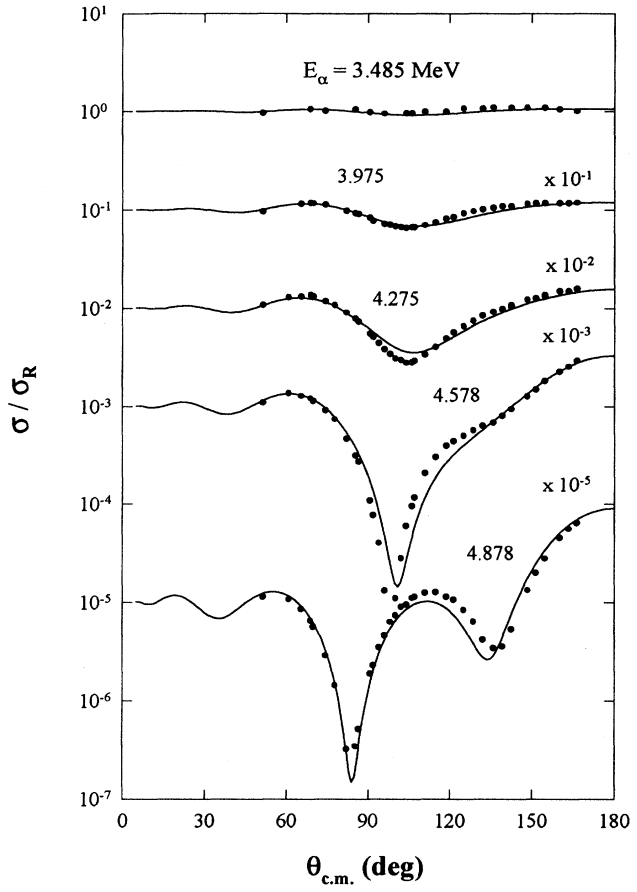

FIG. 6. Comparison of a few selected elastic scattering angular distributions of Buser [26] (dots) with our calculations (solid line).

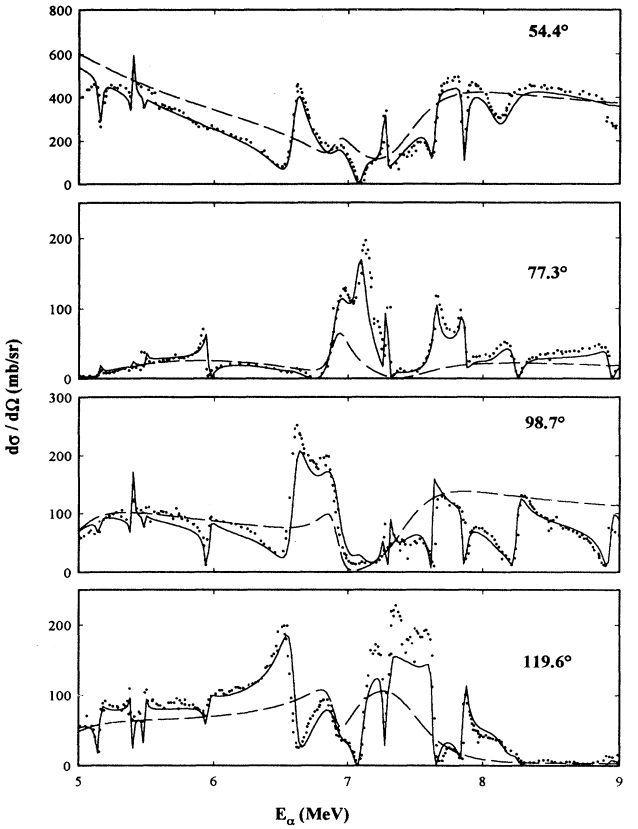

FIG. 7. Same as Fig. 5 for a few selected elastic scattering excitation functions of John *et al.* [19] at $\theta_{\text{c.m.}} = 54.4$, 77.3, 98.7, and 119.6°.

picture in Ref. [18]; Fig. 6 illustrates the merits of the present parametrization for the same data. Figure 5 also shows that the sharp resonances which have to be added to the potential background to reproduce the data in a quantitative way do not alter the underlying gross structure observed in experiment, such as the deep minimum at $\theta_{\text{c.m.}} = 90°$ seen around $E_\alpha \simeq 4.7$ MeV and the broad bump at $\theta_{\text{c.m.}} = 168.9°$ centered around $E_\alpha \simeq 5$ MeV, which are essentially due to the broad $\ell = 0$ and $\ell = 2$ resonances which dominate the scattering in this energy range (cf. Fig. 1).

More spectacular is the agreement obtained above 5 MeV with the excitation functions of John *et al.* [19]. These were measured at many angles ranging from 54.4 to 176.8°; only half of these angles are reported in Figs. 7 and 8. Again the solid lines give the results of the present parametrization, while the dashed lines give the potential contribution to the cross section. It should be noted that the relatively less precise agreement obtained around 7.5 MeV should not be attributed to a defect of our approach since it is also observed in the original phase shift analysis [19]. Some of the comments made in the 3.5 to 5 MeV energy range can be repeated here, although the importance of the nonpotential contributions is obviously growing rapidly with the incident energy. Indeed the average behavior of the excitation functions is still reasonably well described by the potential contribution, but around particular incident energies/angles, some nonpotential resonances have a dramatic influence on the scattering; this is, for example, the case for the $J^\pi = 4^+$, $E_\alpha = 6.60$ MeV resonance. The potential contribution is still dominated by the $\ell = 0$ and $\ell = 2$ resonances in the low-energy range, then by the sharp $\ell = 5$ resonance centered at about 6.9 MeV, which is the third member of the $K^\pi = 0^-$ rotational band, and by the broad $\ell = 4$ resonance at $E_\alpha \simeq 7.3$ MeV, which like the $\ell = 0$ and $\ell = 2$ resonances belongs to the $K^\pi = 0_4^+$ higher nodal rotational band.

The good quantitative agreement obtained here makes possible a reappraisal of the parameters found in the literature for the positions/widths of the resonances of the $K^\pi = 0_4^+$ higher nodal band. For very broad resonances it is difficult to give an unambiguous definition of the resonance width [38]; we will define the resonance width as

$$\Gamma_\ell = \frac{2}{[d\delta_\ell/dE]_{E=E_R}}, \tag{5}$$

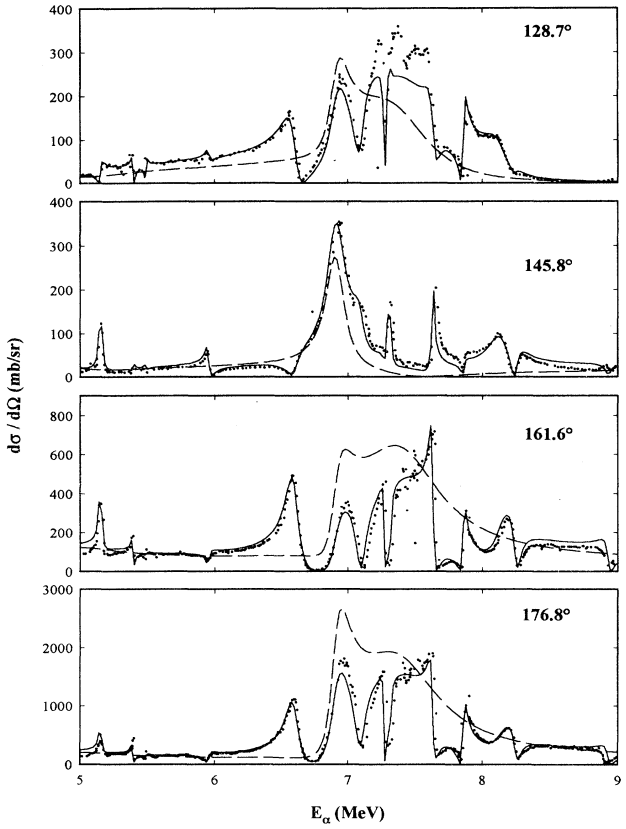

FIG. 8. Same as Fig. 7 for $\theta_{\text{c.m.}} = 128.7$, 145.8, 161.6, and 176.8°.

where E_R is the energy where the slope of the phase shift assumes its maximum value. The resonance parameters obtained are reported in Table III. The parameters of the resonances estimated in this way are somewhat more precise than the values reported in the literature [28]. Indeed the published widths of the $\ell = 0$ and $\ell = 2$ resonances are still those given by McDermott *et al.* [27], whereas account was taken here of the more recent phase shifts deduced by Buser [26]. On the other hand, the width currently reported [28] for the $\ell = 4$ member of the rotational band turns out to be substantially too small with respect to that deduced from the subtracted phase shift and from our potential model; indeed instead of $\Gamma_{\text{c.m.}} = 349$ keV [19, 28] we find $\Gamma_{\text{c.m.}} \simeq 650$ keV, a value much more in line with the widths of the first two members of this band. Incidentally this provides the hint that the $J^\pi = 6^+$ member of the same band, which has been located at many different energies (see, e.g., Ref. [26]) and is no more reported in the recent compilation [28], should most probably not be sought among narrow objects like the previously reported $E_\alpha = 9.79$ MeV resonance with its width of 88 keV [39], the more so as all the potential model and RGM-like calculations predict a width of at least several hundred keV for this resonance. Moreover, the optical model analysis of Ref. [20] revealed that the $J^\pi = 8^+$ member of the $K^\pi = 0_4^+$ band corresponds to the broad bump ($\Gamma > 1$ MeV) seen in the elastic scattering excitation functions of Hunt *et al.* [32] and of Bergman and Hobbie [33] around $E_\alpha = 20$ MeV, confirming earlier results of Ohkubo *et al.* [40], and the (last) $J^\pi = 10^+$ member of the same band is expected to fall around $E_x = 29$ MeV with a width of several MeV [41].

TABLE III. Parameters of the first members of the $K^\pi = 0_4^+$ "higher nodal" rotational band and of the $J^\pi = 5^-$ member of the $K^\pi = 0^-$ "inversion doublet" band extracted from the present analysis.

J^π	E_α (MeV)	E_x (MeV)	$\Gamma_{\text{c.m.}}$ (MeV)
0^+	4.6	8.4	~ 1.3
2^+	4.9	8.7	~ 0.65
4^+	7.4	10.7	~ 0.65
5^-	6.91	10.26	0.136

The only member of the $K^\pi = 0^-$ "inversion doublet" band falling in the investigated energy range is the $J^\pi = 5^-$ state; the parameters of this $\ell = 5$ resonance are also given in Table III. The first two members of this band are in fact seen in elastic scattering at $E_\alpha = 1.3174$ and 3.0382 MeV, with widths $\Gamma_{\text{c.m.}} = 28$ eV and 8.1 keV, respectively [28]. Table II shows that a slight barrier effect ($V_G = 0.5$ MeV) is also needed for obtaining a correct width for the $\ell = 5$ resonance. Use of the A_0 potential, even after tuning the parameter α which controls its depth, indeed slightly overestimates this width, as it does also for the $\ell = 1$ and $\ell = 3$ members of the same band [30]. The optimal reproduction of the $\ell = 1$ and $\ell = 3$ experimental resonance parameters (energy, width) is obtained with depth parameters α differing slightly from those given in Table II; this is not surprising since the latter reproduce at best the average subtracted phase shifts between 3.5 and 9 MeV without introducing any explicit energy dependence, and are thus optimal at midrange, that is, around 6 MeV incident energy. The values obtained, together with the associated volume integrals per nucleon pair, are reported in Table IV. The volume integrals reported in Table IV are somewhat smaller than those of Table II; this points to a further decrease of the volume integrals towards very low energies, at a pace (a few MeV fm^3 per MeV) similar to that predicted by most calculations [7, 21]. Figure 9 compares the experimental excitation function of MacArthur *et al.* [42] at $\theta_{\text{c.m.}} = 160°$ with the predictions of the calculation using the potential parameters of Table IV; the experimental data, which were supplied in arbitrary units [42], have been normalized to the theoretical cross section.

Inspection of Figs. 7 and 8 also shows that the broad structure seen at back angles around 8.6 MeV incident energy, which is reported for a long time as a possible $J^\pi = 2^+$ candidate with a c.m. width of some 500 keV [39, 28], is in fact a region of incident energies, probably the last one, where potential scattering is nearly free from outside nonpotential resonances. This bump appears because of the interference of the smoothly varying potential background with two sharp $\ell = 2$ resonances located

TABLE IV. Parameters and volume integrals per nucleon pair of the modified A_0 potential reproducing the energies and widths of the $J^\pi = 1^-$ and 3^- members of the $K^\pi = 0^-$ rotational band.

J^π	E_α (MeV)	E_x (MeV)	α	V_G (MeV)	j_U (MeV fm^3)
1^-	1.317	5.787	3.2876	1.0	373.6
3^-	3.038	7.164	3.3142	1.0	375.6

at $E_\alpha = 8.246$ and 8.930 MeV with widths $\Gamma_{c.m.} = 53$ and 46 keV, respectively [19, 28]. Comparison (Fig. 10) of the experimental angular distribution [19] at $E_\alpha = 8.5$ MeV with the predictions of our model (solid line) and with the pure potential contribution (dashed line) confirms that the nonpotential resonant contribution plays a minor role in the good agreement obtained with the experimental data. The same figure, which also displays angular distributions at the selected energies $E_\alpha = 5.5$, 6.5, and 7.5 MeV, shows that this is not the case at all the incident energies; for example at 6.5 MeV the potential contribution is seen to interfere severely with the $J^\pi = 4^+$, $E_\alpha = 6.60$ MeV nonpotential resonance.

On the other hand, it is seen that the backward rise seen in experiment at 7.5 MeV, which is well reproduced by the calculation, and also reasonably well by the potential contribution, is dominated by the broad $\ell = 4$ potential resonance (cf. Fig. 8). The relative importance of the various partial waves in the building up of the potential contribution at the most forward and backward angles measured by John *et al.* [19] ($\theta_{c.m.} = 54.4$ and 176.8°) can be appreciated more clearly in Fig. 11; in this figure, we have plotted the cross sections calculated by adding the contribution of the potential phase shift with the indicated ℓ value to the Coulomb scattering amplitude. It can be seen in this way that the characteristic pattern observed at $\theta_{c.m.} = 54.4°$ (thick solid line) is essentially due to the strong interference between the Coulomb amplitude and the contribution of the $J^\pi = 4^+$ member of the $K^\pi = 0_4^+$ rotational band, whereas at $\theta_{c.m.} = 176.8°$ the broad complex structure which dominates the scattering between 6.8 and about 8 MeV incident energies is mainly due to the constructive interference of the contributions of the same state with that of the $J^\pi = 5^-$ member of the $K^\pi = 0^-$ inversion doublet band (contaminated by several narrow $\ell = 2$, 3, and 4 resonances with widths of a few tens keV [19]).

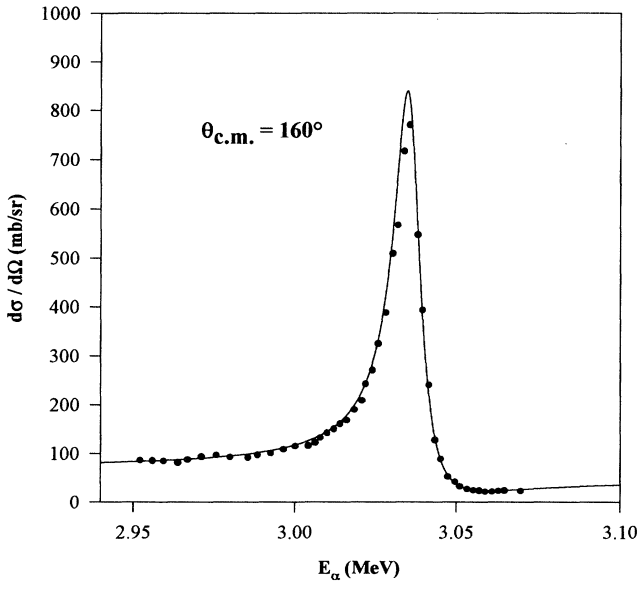

FIG. 9. Comparison of the experimental excitation function of Ref. [42] near the energy of the $E_x = 7.164$ MeV, $J^\pi = 3^-$ resonance of the $K^\pi = 0^-$ inversion doublet band, and the potential model calculations (with $\alpha = 3.3142$ and $V_G = 1.0$ MeV).

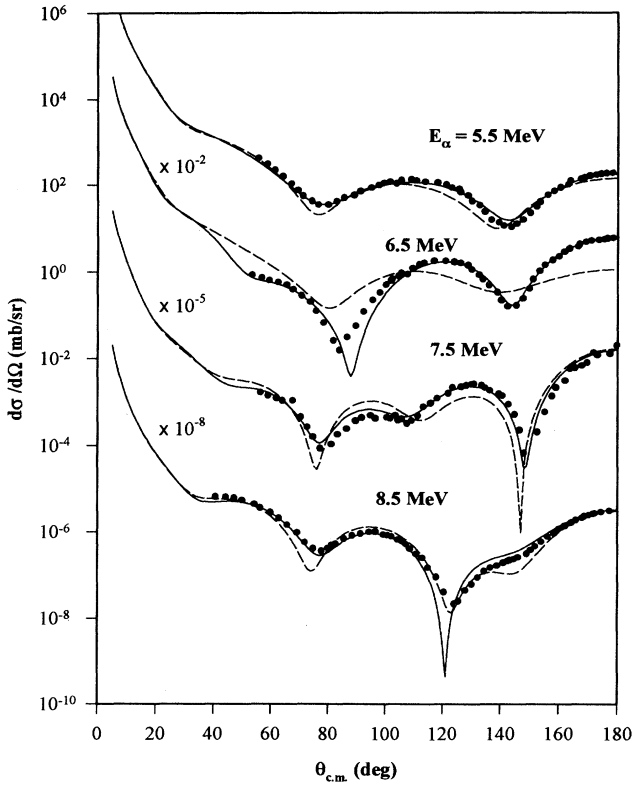

FIG. 10. Comparison of a few selected angular distributions of John *et al.* [19] (dots) with our calculations; the dashed lines present the pure potential contribution.

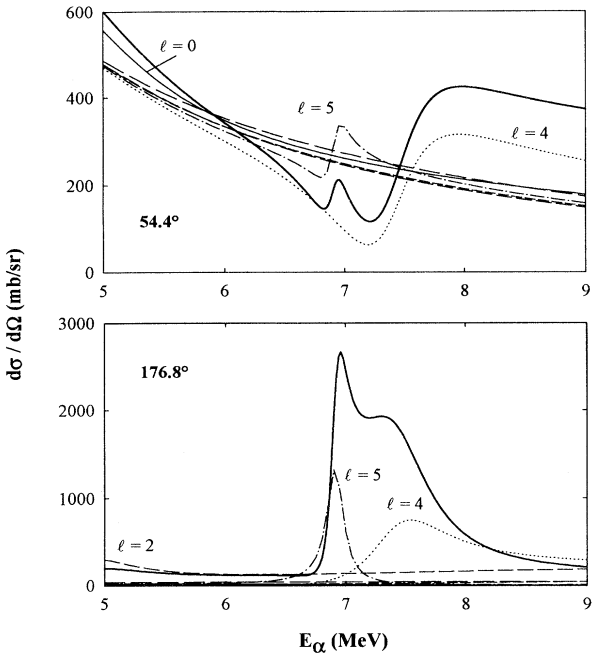

FIG. 11. Contribution of various partial waves to the pure potential excitation functions calculated at $\theta_{c.m.} = 54.4$ and 176.8° (thick solid line: total potential contribution).

E. Ground state band

Additional indications on the validity of the potential picture at low and even negative energies can be gained by turning to the potential predictions for the members of the $K^\pi = 0_1^+$ ^{20}Ne ground state rotational band. Of course it should be borne in mind that although we succeeded in reproducing the data between 3.5 and 9 MeV using an energy-independent (but angular-momentum dependent) potential, naively extending the potential predictions down to negative energies without taking into account any energy dependence — in a region where all the available model calculations predict fast changes such as an additional barrier increase — is not expected to be a realistic approach. An indication that such an energy dependence should be taken into account was provided by the slight decrease of the depth parameter α with respect to the values given in Table II found necessary to reproduce the properties of the first two members of the $K^\pi = 0^-$ rotational band mentioned above (see Table IV). As was the case for these states, we did not attempt to modify the barrier height parameter V_G, since the number of physical quantities available (rms radius of the ground state, $B(E2)$ intraband quadrupole transition probabilities) is too small to guarantee a meaningful determination of the additional free parameters. Therefore we again simply adjusted the parameter α in order to bring the calculated energies of the $J^\pi = 0^+, 2^+$, and 4^+ states of the g.s. band in agreement with the experimental values, while keeping the V_G parameter at the values listed in Table II (we did not include the 6^+ and 8^+ states of this band in the analysis since the $\ell = 6$ and $\ell = 8$ potentials are not determined by the scattering data analyzed here). The parameters obtained are given in Table V, together with the rms radii and the $B(E2)$ intraband quadrupole transition probabilities. The rms radius obtained for the 0^+ state makes possible the calculation of the ^{20}Ne ground state charge radius from [23]

$$\langle r^2 \rangle_{\rm Ne} = \frac{4}{25}\langle r^2 \rangle + \frac{1}{5}\langle r^2 \rangle_\alpha + \frac{4}{5}\langle r^2 \rangle_{\rm O}, \tag{6}$$

where the quantities appearing in the right-hand side (RHS) are the mean square radius of the wave function and the mean square charge radii of the α particle and of ^{16}O, respectively. Using $\langle r^2 \rangle_\alpha^{1/2} = 1.674$ fm [43] and $\langle r^2 \rangle_{\rm O}^{1/2} = 2.72$ fm [43], we find from the calculated value ($\langle r^2 \rangle^{1/2} = 3.757$ fm, cf. Table V) $\langle r^2 \rangle_{\rm Ne}^{1/2} = 2.956$ fm, that is, a result not far from the experimental value (3.004 fm [44]), albeit somewhat too small. One may of course wonder at this stage whether quantities whose calculation involves the wave function on the whole radial range, and not only its asymptotic behavior like in the calculation of the phase shifts and widths, can be quantitatively calculated from a simple local potential approach. One knows for example that the wave functions resulting from RGM microscopic calculations differ at small distances from those obtained from the local equivalent potentials; this is generally known as the "Perey effect." For light systems like α+^{16}O this effect is generally relatively small, but it tends to increase at low energy because its importance is linked to that of the energy dependence of the local equivalent potential $V^{\rm eq}$ [2]; indeed Horiuchi has shown that the Perey factor $\tilde{F}(r)$ by which the local potential wave function should be multiplied in order to reproduce the microscopic wave function is given by [2]

TABLE V. Parameters, volume integrals per nucleon pair, rms radii of the wave functions, and $B(E2)$ values for the modified A_0 potentials reproducing the energies of the $J^\pi = 0^+$ to 4^+ members of the ground state $K^\pi = 0_1^+$ rotational band.

J^π	E (MeV)	E_x (MeV)	α	V_G (MeV)	j_U (MeV fm^3)	$\langle r^2 \rangle^{1/2}$ (fm)	$B(E2)(J \to J-2)$ (e^2 fm^4) th.	expt.
0^+	-4.734	0.	3.174	2.5	340.5	3.757	-	-
2^+	-3.100	1.634	3.094	2.0	342.7	3.790	41	65 ± 3
4^+	-0.486	4.248	3.043	2.0	338.9	3.743	55	71 ± 6

$$\tilde{F}(r) = \sqrt{1 - \frac{\partial V^{eq}(r)}{\partial E}}. \quad (7)$$

At low energy the energy behavior of the local equivalent potential due to antisymmetrization effects implies that at small r, $\tilde{F}(r)$ must be smaller than unity, while it becomes larger than 1 in the surface region. Therefore, quantities sensitive to the large distance behavior of the wave function, like rms radii and $B(E2)$ transition probabilities, could be somewhat underestimated when calculated with a local potential since the local potential wave function tends to be overestimated at small r.

Inspection of the $B(E2)$ values obtained here (Table V) confirms this interpretation, since the calculated values are also somewhat lower than their experimental counterparts (an effective charge $e_{\rm eff} \simeq 1.15$–$1.20\ e$ would be needed to bring the calculated and experimental values in quantitative agreement). In a sense the better agreement obtained in simple potential models where the rapid energy dependence of the potential shape at low energy is not taken into account [30, 25] (the effective charge needed in these calculations is often nearly equal to the bare charge) is somewhat fortuitious, since neglecting the barrier increase enhances the wave function in the surface region and mocks up to some extent the Perey effect; this point has been emphasized by Wada and Horiuchi [10].

Taking the parameters of Table V at their face values, we can also calculate the volume integrals of the potentials reproducing the energies of the states of the ^{20}Ne ground state band in order to obtain additional indications on the main trends of the energy dependence of the potential when energy decreases. Our calculations point to a further decrease of the volume integrals, at a pace of some 4 to 8 MeV fm^3 per MeV between $E_{\rm c.m.} \simeq 4$ MeV and $E \simeq -5$ MeV (for $\ell = 0$ for example, one had $j_V = 380.8$ MeV fm^3, cf. Table II, to be compared to the value $j_V = 340.5$ MeV fm^3 obtained here at $E = -4.73$ MeV; the $E_\alpha = 32.2$ MeV A_0 potential has $j_V = 399.1$ MeV fm^3). This value, although rather large, is not inconsistent with the results of the theoretical calculations referred to above: indeed a significant energy dependence is predicted for the α+^{16}O system by both antisymmetrization and dispersion relation effects in this energy range, and as these two mechanisms have a different physical origin they are expected to be additive to some extent. Still in view of the uncertainties pointed out above in extracting the parameters of the potential at these low energies, the trends observed here should only be taken as purely qualitative indications on the ultimate fate of the α+^{16}O potential at very low energy.

III. SUMMARY AND CONCLUSIONS

A systematic analysis of the existing $^{16}O(\alpha,\alpha)$ elastic angular distributions and excitation functions for incident energies ranging from 3.5 to 9 MeV makes possible the extraction of real, energy-independent potentials for angular momenta ranging from 0 to 5. These potentials give a precise description of the elastic scattering data when the potential background they generate is supplemented with the resonant nonpotential contributions, that is, the contribution of the resonances which do not have a single-particle character. Our study makes possible the extraction of the purely potential contribution to the scattering, which is found to explain well the gross structure underlying the experimental data; however, inclusion of the nonpotential resonant contributions is important to get quantitative agreement with experiment, and it would thus have been very difficult to extract meaningful information on the underlying α+^{16}O interaction by restricting to a description of the average behavior of the data.

The potentials obtained here confirm the results of a previous study by the same authors [18], that is, the need of introducing a slight angular momentum dependence, and a significant enhancement of the barrier height with respect to the global potential (A_0) extracted from an extensive optical model analysis of $^{16}O(\alpha,\alpha)$ elastic data between 20 and 150 MeV [20]; inside the barrier the low-energy potentials are on the contrary found to be more attractive than the higher-energy potential. The rather precise information obtained here for the radial dependence of the potential should be useful in clarifying the relative importance for light systems of various mechanisms, like antisymmetrization or dispersion relation effects, which have been invoked in the literature to explain the low-energy features of the interaction.

The more precise study carried out here reveals that the barrier enhancement decreases with angular momentum, which was expected since the low-energy potentials must eventually converge towards the A_0 potential when energy, and thus the angular momentum of the dominant partial waves, increases. The barrier enhancement is also found to be significantly parity dependent, the rise of the barrier found for odd partial waves being smaller than that needed for even partial waves; below about 5 fm the even potentials are on the contrary deeper than their odd counterparts (see Fig. 12, where the poten-

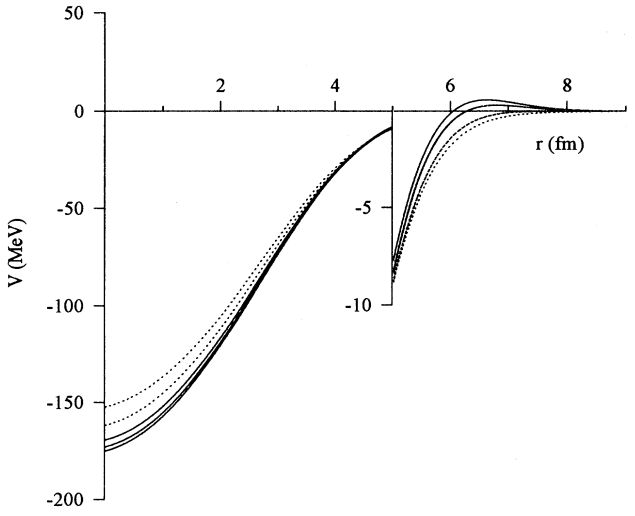

FIG. 12. Nuclear potentials obtained for odd ℓ (dotted lines) and even ℓ (solid lines) (cf. Table II).

tials corresponding to the two parities have been plotted separately). Although this feature may sound rather unconventional, it may not be at variance with the microscopic calculations since, although these calculations predict little parity dependence in this mass region, the importance of parity dependence is expected to grow at low energy. It would thus be worth reinvestigating this effect more quantitatively within the frame of microscopic approaches like the resonating group method, the more so as detailed studies of this effect at very low energy are rather scarce. To obtain meaningful information on the parity dependence of the potential from these calculations, one must be able to build local potentials which are phase equivalent to the nonlocal RGM kernels. One of the most powerful methods to perform this construction relies on the WKB approximation [2], which tends to lose its accuracy at low energy [45]; therefore other techniques like those relying on potential inversion might be useful in this energy region. It is worth pointing out in this respect that a recent study of Mackintosh and Cooper [46], in which the local potentials corresponding to the various exchange components in the RGM calculations of LeMere *et al.* [47] for the $\alpha+^{16}$O system are determined by a potential inversion technique, points to the fact that the four-particle exchange contribution induces a sizable parity dependence in the inverted potential; it would be worth repeating this type of calculations using RGM results at lower energies where stronger effects are expected.

The potentials extracted reproduce the properties of the first three members of the ^{20}Ne $K^\pi = 0^+_4$ "higher nodal" rotational band, which dominate the scattering in the investigated energy range. The width ($\Gamma_{\text{c.m.}} = 650$ keV) of its $J^\pi = 4^+$ member, which is located at $E_x = 10.7$ MeV, is found to be substantially larger than that usually reported in the literature, pointing to the fact that the widths of the members of this band do not decrease dramatically with J, and that the (still unknown) $J^\pi = 6^+$ state of this band should be searched among rather broad objects.

The properties of the first members of the $K^\pi = 0^-$ "inversion doublet" band (the $J^\pi = 5^-$ state is the only member of this band falling in the investigated energy range) are also nicely reproduced if account is taken of the energy dependence of the potentials when energy decreases. Those of the $K^\pi = 0^+_1$ ground state band are also qualitatively reproduced provided allowance is made for a substantial decrease of the strength of the potential at very low energies; however the limitations of a purely local potential approach become apparent here, since quantities derived from the full range wave functions, such as rms radii and $B(E2)$ transition probabilities, are found to be somewhat underestimated, most probably as a consequence of the so-called Perey effect.

ACKNOWLEDGMENTS

F.M. and G.R. are very grateful to Prof. R. Ceuleneer for his continuous interest and support, and to Dr. S.G. Cooper, Dr. R.S. Mackintosh, and Dr. P. Mohr for useful and interesting discussions.

[1] G.R. Satchler, Phys. Rep. **199**, 147 (1991).
[2] H. Horiuchi, in *Trends in Theoretical Physics*, edited by P.J. Ellis and Y.C. Tang (Addison-Wesley, Reading, MA, 1991), p. 277.
[3] *Proceedings of the Workshop on Heavy Ion Collisions at Energies near the Coulomb Barrier*, Daresbury, U.K., 1990, edited by M.A. Nagarajan, Institute of Physics Conference Series, No. 10 (Institute of Physics, Bristol, 1991).
[4] W. Reisdorf, J. Phys. G **20**, 1297 (1994).
[5] M.A. Nagarajan, C.C. Mahaux, and G.R. Satchler, Phys. Rev. Lett. **54**, 1136 (1985).
[6] C. Mahaux, H. Ngô, and G.R. Satchler, Nucl. Phys. **A449**, 354 (1986).
[7] C. Mahaux, H. Ngô, and G.R. Satchler, Nucl. Phys. **A456**, 134 (1986).
[8] T. Matsuse, M. Kamimura, and Y. Fukushima, Prog. Theor. Phys. **53**, 706 (1975).
[9] K. Aoki and H. Horiuchi, Prog. Theor. Phys. **68**, 2028 (1982).
[10] T. Wada and H. Horiuchi, in *Proceedings of the Fifth International Conference on Clustering Aspects in Nuclear and Subnuclear Systems*, Kyoto, Japan, 1988, edited by Y. Sakuragi, T. Wada, and Y. Fujiwara, contributed papers (Physical Society of Japan, Tokyo, 1989), p. (iii)-36.
[11] E.W. Schmid, S. Saito, and H. Fiedeldey, Z. Phys. A **306**, 37 (1982).
[12] R. Lipperheide, H. Fiedeldey, E.W. Schmid, and S.A. Sofianos, Z. Phys. A **320**, 265 (1985).
[13] W.G. Love, T. Terasawa, and G.R. Satchler, Nucl. Phys. **A291**, 183 (1977).
[14] J.S. Lilley, B.R. Fulton, M.A. Nagarajan, I.J. Thompson, and D.W. Banes, Phys. Lett. **151B**, 181 (1985).
[15] Y. Kondō, F. Michel, and G. Reidemeister, Phys. Lett. B **242**, 340 (1990).
[16] G.R. Satchler, in Ref. [3], p. 109.
[17] N. Vinh Mau, in Ref. [3], p. 1.
[18] F. Michel, Y. Kondō, and G. Reidemeister, Phys. Lett. B **220**, 479 (1989).
[19] J. John, J.P. Aldridge, and R.H. Davis, Phys. Rev. **181**, 1455 (1969).
[20] F. Michel, J. Albinski, P. Belery, Th. Delbar, Gh. Grégoire, B. Tasiaux, and G. Reidemeister, Phys. Rev. C **28**, 1904 (1983).
[21] T. Wada and H. Horiuchi, Phys. Rev. Lett. **58**, 2190 (1987).
[22] S. Yamaguchi, K. Yabana, and H. Horiuchi, Prog. Theor. Phys. **82**, 53 (1989); **82**, 217 (1989).
[23] B. Buck, C.B. Dover, and J.P. Vary, Phys. Rev. C **11**, 1803 (1975).
[24] Y. Fujiwara, H. Horiuchi, K. Ikeda, M. Kamimura, K. Kato, Y. Suzuki, and E. Uegaki, Suppl. Prog. Theor.

Phys. **68**, 29 (1980).
[25] H. Abele and G. Staudt, Phys. Rev. C **47**, 742 (1993).
[26] M. Buser, Helv. Phys. Acta **54**, 439 (1981); M. Buser, Ph.D. Thesis, Univ. Basel, 1980 (unpublished).
[27] L.C. McDermott, K.W. Jones, H. Smotrich, and R.E. Benenson, Phys. Rev. **118**, 175 (1960).
[28] F. Ajzenberg-Selove, Nucl. Phys. **A475**, 1 (1987).
[29] H. Horiuchi and K. Ikeda, Prog. Theor. Phys. **40**, 277 (1968).
[30] F. Michel, G. Reidemeister, and S. Ohkubo, Phys. Rev. C **37**, 292 (1988).
[31] J.R. Cameron, Phys. Rev. **90**, 839 (1953).
[32] W.E. Hunt, M.K. Mehta, and R.H. Davis, Phys. Rev. **160**, 782 (1967).
[33] C. Bergman and R.K. Hobbie, Phys. Rev. C **3**, 1729 (1971).
[34] D.A. Goldberg and S.M. Smith, Phys. Rev. Lett. **29**, 500 (1972).
[35] D.M. Brink and N. Takigawa, Nucl. Phys. **A279**, 159 (1977).
[36] F. Michel and R. Vanderpoorten, Phys. Rev. C **16**, 142 (1977).
[37] Th. Delbar, Gh. Grégoire, G. Paic, R. Ceuleneer, F. Michel, R. Vanderpoorten, A. Budzanowski, H. Dabrowski, L. Freindl, K. Grotowski, S. Micek, R. Planeta, A. Strzalkowski, and K.A. Eberhard, Phys. Rev. C **18**, 1237 (1978).
[38] A. Arima and S. Yoshida, Nucl. Phys. **A219**, 465 (1974).
[39] F. Ajzenberg-Selove, Nucl. Phys. **A392**, 1 (1983).
[40] S. Ohkubo, Y. Kondō, and S. Nagata, Prog. Theor. Phys. **57**, 82 (1977).
[41] F. Michel, G. Reidemeister, and S. Ohkubo, Phys. Rev. C **35**, 1961 (1987).
[42] J.D. MacArthur, H.C. Evans, J.R. Leslie, and H.-B. Mak, Phys. Rev. C **22**, 356 (1980).
[43] R.C. Barrett and D.F. Jackson, *Nuclear Sizes and Structure* (Clarendon, Oxford, 1977).
[44] E.A. Knight, R.P. Singhal, R.G. Arthur, and M.W.S. Macauley, J. Phys. G **7**, 1115 (1981).
[45] S. Ait-Tahar, R.S. Mackintosh, S.G. Cooper, and T. Wada, Nucl. Phys. **A562**, 101 (1993).
[46] R.S. Mackintosh and S.G. Cooper, Nucl. Phys. A (to be published).
[47] M. LeMere, D.J. Stubeda, H. Horiuchi, and Y.C. Tang, Nucl. Phys. **A320**, 449 (1979).